

THERMAL DYNAMIC BEHAVIOR OF SINGLE COMPONENT: EXPERIMENTAL ANALYSIS AND NUMERICAL MODELING

Paolo BAGGIO¹, Alessandro PRADA²

In the present paper the comparison between the results obtained by an extended series of measurements on a composite element in transient regime are presented. Temperatures and heat fluxes have been collected by means of thermocouples and heat flux meter during the summer of 2009. A critical analysis of data collected is presented and the results point out the high importance of radiation heat transfer through roof in summer period.

Keywords: envelope, RBS, unsteady state, roof behavior.

1. Introduction

In the last few years, energy use has increased due to cooling systems, such as split and packaged units. Consequently, the awareness of improving the performance of building envelope has grown.

The first step to reduce the cooling loads is the limitation of the heat fluxes entering through the envelope. This is possible if the building components are correctly designed. Solar gains, in residential buildings, are the most important cooling loads and, in this respect, due to the high exposition to solar radiation, the roof surface can be an important factor (in addition to glazed surfaces). In fact, in southern Europe the roof surface temperature can often rise up to 70÷80°C [1]: according to that, during the experimental tests, the authors measured temperature values around 70°C in the test area located in northern Italy.

During the summer season, a well designed envelope should limit the unsteady state heat flux both with a shift in time of the peak load and with a reduction of the heat amplitude. Unfortunately, to achieve high values of these parameters (as defined by the EN ISO 13786 standard), an heavy mass layer is usually required, increasing the structure costs and causing problems in seismic regions. In order to avoid that, it is possible to use a double-skin ventilated roof to reduce the solar gains through the roof, and consequently, the cooling load. The net effect of this passive strategy on the energy consumption, on overheating and on thermal comfort can be quite significant. In fact, the airflow in the ventilation

¹ Full Prof., Engineering Faculty, Civil and Environ. Dep., University of Trento, Italy

² PhD student, Engineering Faculty, Civil and Environ. Dep., University of Trento, Italy

channel, due to buoyancy force and to wind effect, removes a fraction of the heat flux due to solar radiation reducing the heat transfer toward the inside part of the building. If the ventilated double skin is coupled with a radiant barrier (RBS), the radiation heat transfer between the surfaces of the ventilation channel can be further decreased: for example, by means of a RBS it is possible to obtain a reduction of the total heat transfer ranging from about 40÷45% for a roofing structure having a thermal resistance value of 1.95 [$\text{m}^2\text{K W}^{-1}$] to approximately 15÷20% when the resistance is equal to 5.28 [$\text{m}^2\text{K W}^{-1}$] of the insulation [2].

Many authors have experimentally and analytically investigated the thermal behavior of double-skin structures. Different methods have been proposed to establish an intrinsic characterization of radiant barriers, but a specific International Standard is still lacking, because of the difficulty of finding a simple and agreed upon approach.

In the present paper an extended series of experimental data collected on a full scale component in transient regime are presented. The experimental tests have been carried out on two real buildings with the same exposure and inclination angle, differing for the layers stratigraphy of the component analyzed. In first roof the design strategy was an high thermal insulation thickness (14 cm) coupled with a ventilation chamber. In the second roof insulation thickness (12 cm) and ventilation layer hinders the heat flux through conduction. In additions to this layer a reflective sheet was installed in order to minimize the heat transfer by radiation. The surface temperature and inward heat flux values measured continuously both on the internal and external side of an opaque representative component have been used as boundary conditions for the energy simulations by a RC network scheme.

2. Experimental Analysis

The experimental tests have been carried out on two real ventilated pitched roofs during the summer of 2009 in Levico Terme (Trento, Italy). The authors selected two ventilated roofs; in both cases the roof is 7 meters long, its orientation faces south-west and the roof pitch is equal to 27 degrees.

The first roof (roof A) had a covering made of concrete tile and a wood bearing structure. The second roof (roof B) had clay tiles and the same beneath structure. The two roofs differing only for the insulation thickness (12 cm for roof A and 14 cm for roof B) and for the presence in the roof A of a reflective layer over the ventilation channel.

In Figure 1 the roof layer structure is illustrated. A waterproof membrane is placed under the black tiles. In case A (roof with radiant barrier) the underlying structure is an oriented strand board (OSB) panel and its inferior part is covered by a reflective aluminum sheet. In case B (roof without radiant barrier), instead,

an OSB panel, without reflective sheet, is used. The last three layers are the ventilation channel (6 cm of thick), an insulating layer of extruded polystyrene foam XPS (12 cm in roof A and 14 cm in roof B) and plasterboard (1.5 cm thick).

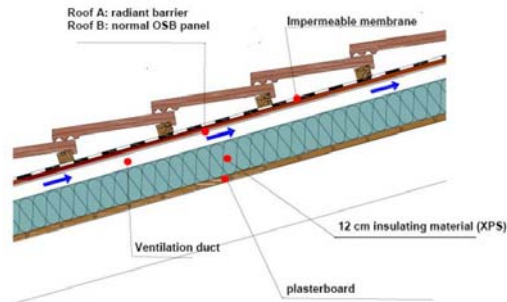


Fig. 1. Cross section of the two roof analyzed

The following reference conditions have been assumed in calculations:

Table 1. Physical propriety of the roof covering surfaces.

Tile propriety	Roof A	Roof B
material	concrete	clay
thickness	1.5 cm	2.5 cm
conductivity	$1.5 \text{ W m}^{-2} \text{ K}^{-1}$	$1.0 \text{ W m}^{-2} \text{ K}^{-1}$
density	2100 kg m^{-3}	2000 kg m^{-3}
specific heat	$1000 \text{ J kg}^{-1} \text{ K}^{-1}$	$800 \text{ J kg}^{-1} \text{ K}^{-1}$
Surface emissivity	0.95	0.90
Solar absorptance	0.70	0.70

By means of two thermocouples, the surface temperatures have been measured on the external and internal side in the middle of the roof length. The flow meters were attached to the upper and lower surface of the roof in order to measure the inward and reemitted fluxes of this building structure. These pieces of equipment were connected to a datalogger, and the data were collected every 1 min. The measurement period was 2 months, from July to August 2009.

During the same period, in a closed place, weather data have been measured. The available measured data were air temperature, wind velocity and direction, global solar radiation on 30 degrees tilted surface.

Even if the measurements were taken at different times the roof structures were quite similar and a direct comparison between measurements has been done only when the external boundary conditions were similar.

3. Experimental results

In this paper results for 2 different couple of selected days are presented. For roof A the reference period start data are from the midnight on 27/7/2009 to the midnight on 29/7/2009. Instead, for roof B data presented are from the midnight on 16/8/2009 to the midnight on 18/7/2009.

These days were chosen since they represent a typical summer period with high solar radiation and very low cloudiness.

Figures 2 show solar radiation on 30° tilted surface. Even if these data were collected in a placed close to roof, there are some different boundary conditions. For instance, at 9 AM and 4 PM there were some shadings on the pyranometer but not on the roof.

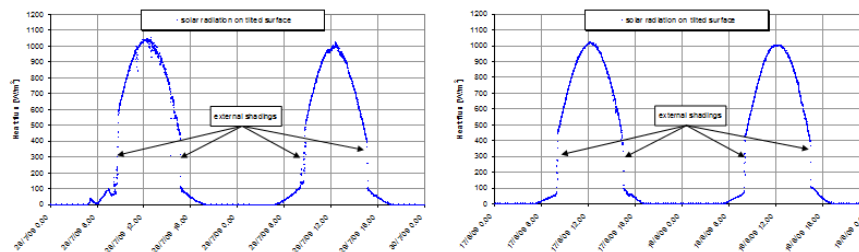


Fig. 2. Solar radiation on tilted surface for roof A (left) and for roof B (right).

Even though this uncertainty, these data show that during selected days roof A and roof B were exposed to the same peak of solar radiation.

With the goal of evaluating the effectiveness of the dynamic behavior of the roof, one of the most interesting data are the temperatures measured just over the waterproof membrane and at the internal surface in an unconditioning space.

The following graphs show temperatures recorded, with a time step of 1 minute, continuously for two days on roof A and on roof B (fig. 3).

Figures 3 show that the shift in time between the peak in the external surface temperature (13.30 PM) and the internal one (15.10 P.M.) is quite similar for both the roof typologies.

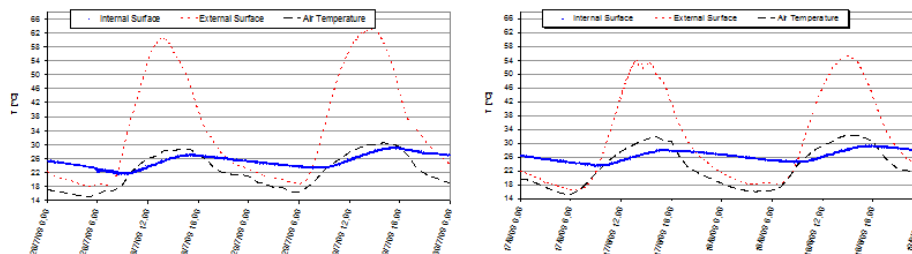


Fig 3 Temperature trend registered on roof A (left) and on roof B (right).

In figure 4, the heat fluxes recorded at the external and internal surface of the roof are plotted.

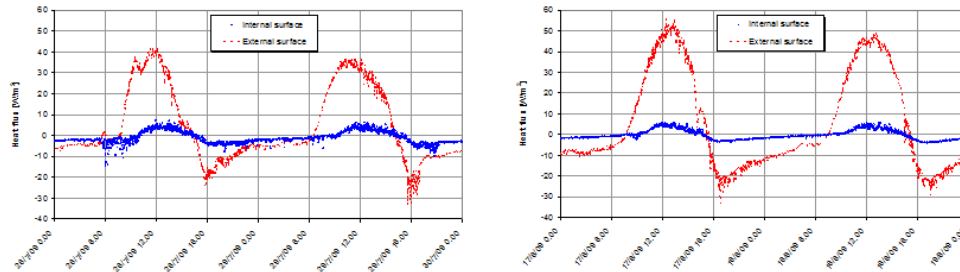


Fig 4 Heat flux trends registered on roof A (left) and on roof B (right).

At the peak time, which occurred at 12:30 h, when the solar radiation was maximum, the inward heat flux for the case A was 40 Wm^{-2} and greater values were recorded in roof B about 53 Wm^{-2} . This increasing occurred due to the high temperature recorded in the second roof and to the different radiation parameter of the tiles surfaces. It was observed that only a 5% of the solar radiation was transfer through the envelope component. This appeared quite strange so a series of numerical simulations were performed in order to evaluate the possible source of uncertainty in the measurements.

The high temperature of the tiles suggested the possibility of the underestimating of the radiation contribute of the heat exchange between the tiles surface and the waterproof membrane.

4. Data Processing

For the evaluation of the reliability of the experimental data collected, heat exchanges on the external surface of the roof are computed with a RC scheme illustrated in figure 5.

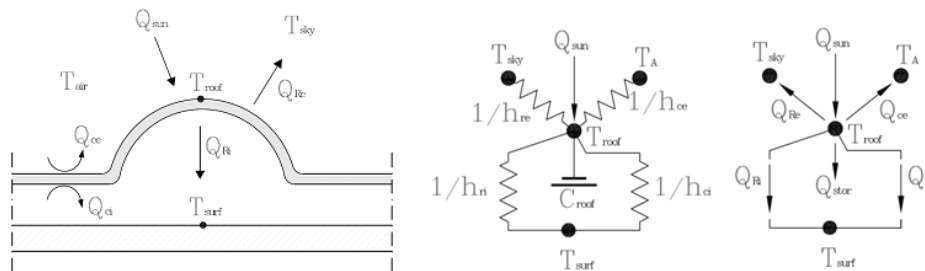


Fig. 5. Heat balance and RC scheme for the heat transfer process.

The thermal network for the physical model considered is shown in figure 5 and the heat balance equations from the thermal network at the point T_{roof} become:

$$Q_{ce} + Q_{re} + Q_{ci} + Q_{ri} - Q_{stor} = Q_{sun} \quad (1)$$

where every single component has been estimated with linearized relationship. Experimental data have been used like input for RC scheme for solar radiation, surface and ambient temperature. For sky temperature, Swinbank's formula [8] has been used. Radiation heat transfer coefficients both for the external and internal surface are given by:

$$h_{re} = \sigma \cdot \varepsilon_{roof} \cdot (T_{roof} + T_{sky}) \cdot (T_{roof}^2 + T_{sky}^2) \quad (2)$$

$$h_{ri} = \frac{\sigma \cdot (T_{roof} + T_{surf}) \cdot (T_{roof}^2 + T_{surf}^2)}{\frac{1}{\varepsilon_{roof}} + \frac{1}{\varepsilon_{surf}} - 1} \quad (3)$$

The external convection heat coefficient was split into forced and natural components [7]. The natural convection component was calculated using the formula proposed by Walton [7], instead of the forced convection component is based on a correlation by Sparrow [6]. By substituting experimental relations into equation (1), the roof surface temperature may be expressed as:

$$T_{roof} = \frac{Q_{sol} - Q_{stor} + h_{ce} \cdot T_A + h_{re} \cdot T_{sky} + (h_{ci} + h_{ri}) \cdot T_{surf}}{h_{ce} + h_{re} + h_{ci} + h_{ri}} \quad (4)$$

This relation is an implicit equation, because of every heat transfer coefficient depend on roof temperature, and should be used in an iterative process to calculate the actual temperature. Equation (4) has been solved performing the heat balance with a time step of 1 minute. The temperatures of the external surface of the roof are presented in figure 6. These pictures show that both for roof A and for roof B the peak temperature is equal to 70 °C, in agreement with Dimoundi [1].

The numerical scheme gives heat fluxes greater than the fluxes measured with flux meter. A possible source of this problem in the data collection is the difference between the emissivity of the instrument and the waterproof membrane.

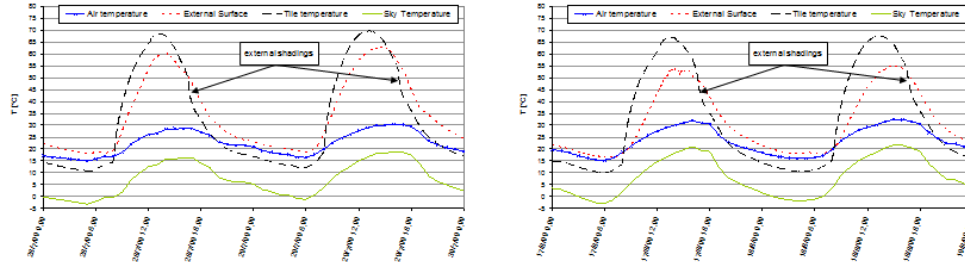


Fig 6 Temperature measured and simulated for roof A (left) and B (right).

Starting from the usual formula (Eq. 2 and 3) for the evaluation of the radiation heat transfer coefficient in a cavity, a correction factor was developed.

Assuming that T_{inst} is equal to T_{surf} , the ratio between the actual and measured radiation heat component is given by:

$$\frac{Q_{ri}}{Q_{rad,mis}} = \frac{1/\varepsilon_{roof} + 1/\varepsilon_{inst} - 1}{1/\varepsilon_{roof} + 1/\varepsilon_{surf} - 1} \quad (5)$$

where ε_{surf} and ε_{inst} are respectively the emissivity of the waterproof membrane and the emissivity of the heat flux meter. These parameters have been estimated with a thermocamera analysis and are equal to 0.90, for the membrane, and 0.55 for the instrument. These value are in strongly agreement with the data suggested in the Mikael's and also in Öhman's database [4,5].

Using the parameter given by (5) for the correction of the radiation part of the heat flux, the trend reported in figure 4 for the two roofs become :

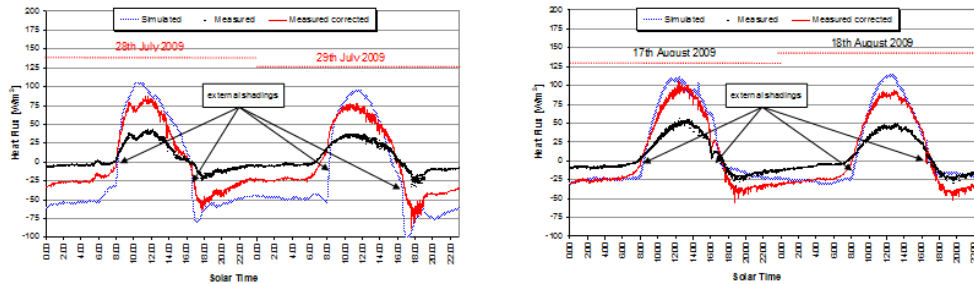


Figure 7 Trend in external heat flux for roof A (left) and B (right).

Figures 7 show a good agreement with the RC model and the data corrected. Moreover, a flux of 100 Wm^{-2} obtained for the peak hour with the correction coefficient agree quite well with previous literature studies.

6. Conclusions

In this paper the thermal dynamic response of a ventilated roof has been analyzed. This study has been done through the comparison of the results obtained by numerical simulation and experimental data. The experimental results about full scale pitched roofs clearly demonstrated the importance of the radiation contribute of heat transfer in the roof component. This importance underline the possibility of reflective radiant barriers in reducing the insulation temperature and, consequently, solar heat gains.

These preliminary results point out similar internal surface temperature for roof A and roof B and also the difference in the heat reemitted by the roof surface into the ambient are negligible. Experimental result seems to affirm that the effect of the reflective foil are of the same magnitude of the thermal insulation of 2 cm of XPS.

Nevertheless, some adjustment to the experimental equipment is still necessary in order to minimize the errors due to the emissivity difference of the instruments. To this purpose, another research activity is currently ongoing.

REFERENCES

- [1]. *A. Dimoudi, A. Androutsopoulos, S. Lykoudis, S.*, "Summer performance of a ventilated roof component", in *Energy & Buildings*, **vol. 38/6**, 2006, pp. 610-617
- [2]. *A.M. Medina, B. Young*, "A perspective on the effect of climate and local environmental variables on the performance of attic radiant barriers in the United States", in *Building and Environment*, **vol. 41/12**, 2006, pp. 1767-1778
- [3]. *F. Miranville, H. Boyer, P. Lauret, F. Lucas*, "A combined approach for determining the thermal performance of radiant barriers under field conditions", in *Solar Energy*, **vol. 82/5**, 2008, pp. 399-410
- [4]. *C. Öhman*, "Emittance measurements using AGEMA E-Box", in *Technical report*, AGEMA, 1999.
- [5]. *A. Mikaél Bramson*, *Infrared Radiation*, in *A Handbook for Applications*, Plenum press, N.Y.
- [6]. *E.M. Sparrow, J.W. Ramsey, E.A. Mass*, "Effect effect of finite width on heat transfer and fluid flow about an inclined rectangular plate", in *Journal of Heat Transfer*, **vol 11**, 1979, pp. 204
- [7]. *G.N. Walton*, "Thermal analysis research program reference manual" in NBSSIR 83-2655. National Bureau of Standard, 1983.
- [8]. *W.C. Swinbank*, "Longwave radiation from clear skies", in *Metrological Society*, **vol1. 89**, 1963, pp.339-348.